

Studying Shear and Discharge Rate of Proteins in Microfluidic Junctions, under Electrokinetic Effects

Babak kamali Doust Azad

Department of Mechanical Engineering,
Iran University of Science and Technology, Iran
E-mail: kamalidostbabak@gmail.com

Sasan Asiaei*

Department of Mechanical Engineering,
Iran University of Science and Technology, Iran
E-mail: Asiaei@iust.ac.ir

Borhan Beigzadeh

Department of Mechanical Engineering,
Iran University of Science and Technology, Iran
E-mail: b_beigzadeh@iust.ac.ir

Received: 24 March 2016, Revised: 18 May 2016, Accepted: 23 May 2016

Abstract: Changes of hydrodynamic parameters in microchannel branches affect the suspended biological samples in blood. To prevent denaturation and hemolysis, we have numerically investigated the effect of divergence angle on shear rate and velocity at branch entrance (discharge rate), under electroosmotic flow. In such flow, hydrodynamic properties are also affected by zeta potential at the microchannel walls. We have also studied the effect of change of zeta potential (ξ) proportion at main channel wall (ξ_1) to that of branch channel (ξ_2), on the discharge rate to find its maximum for different divergence angles. In the divergence angle of 60° and while zeta potential at the branch wall is equal to its value at main channel wall, the tendency of particles to pass through the branch is the highest among all examined degrees. At the zeta potential proportion of ($\xi_1/\xi_2 = 0.5$), the change of divergence angle has almost no effect on the maximum velocity in the branch. In addition, with increase of divergence angle from 60° to 150° , the shear rate at the branch will become 2.1 times higher.

Keywords: Discharge rate, Electrokinetic, Electroosmotic flow, Hemolysis, Microfluidics, Numerical modeling, Protein denaturation, Shear rate

Reference: Kamali Doust Azad, B., Asiaei, S., and Beigzadeh, B., "Studying the Shear and Discharge Rate of Proteins in Microfluidic Junctions, under Electrokinetic Effects", Int J of Advanced Design and Manufacturing Technology, Vol. 9/ No. 4, 2016, pp. 81-87.

Biographical notes: **Sasan Asiaei** received his PhD in Mechanical Engineering from University of Waterloo, 2013. He is currently Assistant Professor at the School of Mechanical Engineering, Iran University of Science and Technology (IUST), Iran. His current research interest includes Microfluidics and Rapid Tests. **Borhan Beigzadeh** is Assistant Professor of Mechanical engineering at the IUST, Iran. He received her PhD in Mechanical engineering from Sharif University of Technology, Iran.. His current research focuses on (Bio-)Robotics, Cognitive Science, and Traditional Medicine. **Babak Kamali** has recently graduated from Mechanical Engineering, Bio-Mechanics from Iran University of Science and Technoogy. His is currently working in the field of Microfluidics and Microfabrication.

1 INTRODUCTION

Electrokinetic flows are a suitable alternative for pressure driven flows in sample transport and fluids transfer in microfluidic systems [1]–[4]. Due to the simple manufacturing process and absence of moving parts, using electrokinetic flows in small channels and microchannels is extremely useful [5],[6]. One of the electrokinetic phenomena which has recently been considerably investigated is electroosmosis [7]. Electroosmotic flows are widely used to transport liquids and separate samples in many biological applications and chemical analytic systems [8]. One of the important implications of electroosmotic flows is in lab on a chip (LOC) devices [9]. Electroosmotic flow in LOC have found many implications in biochemistry, biology and medicine such as drug delivery [10], synthesis and production of various organs [11], cellular analysis [12] and etc.

Many researchers have studied electroosmotic flow for channels with different geometries and conditions [13]–[16]. In all these devices the existence of networks of microchannels is essential, and in most of them, a liquid or biological sample must be driven in a microfluidic network with the following characteristics: delivery on demand, within the required time span, without any pressure disturbances, and without portability problems [17]–[19]. In any microfluidic network, there are microchannels in which various branches with different geometries must be used to merge, manipulate or separate liquids and different biologic samples. Most of this geometries are T-shaped or Y-shaped [20]–[22], and the geometrical properties of the junctions have important hydrodynamic impacts on the fluid flow and the carried particles [23].

There are several reports on the effect of branches' geometry on the fluid flow. Ebrahimi et al. (2014) had a comprehensive study on heat transfer and flow entrainment in T-shaped microchannels under combined pressure-electroosmotic driven flows. Enhanced mixing was achieved due to non-uniform zeta potentials, which pushes the induced vortices into the middle of the channel [20]. In another study, Mansur et al. investigated the efficiency of entrainment in micro mixtures with one and double-sided T-shaped microchannels without any physical/geometrical inclusion [24]. The double-T-mixer was much more efficient compared with the original configuration. The researchers also considered the mixing efficiency with and without static mixing elements (SME), and it was revealed that the increase of mixing efficiency is a function of eddies and lateral velocity components upon flow of mixture through these elements. The latter trend prevails in almost all related studies, nevertheless, the junction angle and its various hydrodynamic impacts are not much dealt-with, and the majority of research papers are focusing on 90° angle, T-shaped branches [13]–[23]. The impact of divergence angle change on the hydrodynamic properties of electroosmotic flow such as shear rate [25], flow discharge

rate and maximum speed at different cross-sections of the microchannel is significantly important, yet to be comprehensively studied. The value of shear rate has a direct impact on the shear stress imposed on the suspended particles in biologic samples [26].

Excessive shear stress may lead to the cell/protein denaturation and for example for red blood cells causes hemolysis in the blood sample [27], [28]. Moreover, the discharge rate, expressed as the tendency of suspended particle to pass through the branch, is related to the divergence angle [29]. In this paper, the effect of divergence angle change on the shear rate at the branch and also the tendency of particles to pass through the branch is investigated. Our results show that increase of divergence angle might lead to attenuated stress levels, and possibly denaturation of the transported proteins, immediate to the junctions. Moreover, by proper adjustment of the surface potential of intersecting microchannel, the impact of the junction angle on the flow velocity in the sectioned channel can be cancelled out.

2 MATHEMATICAL MODEL

Electroosmosis is a phenomenon inherently related to the interaction between fluid and its solid boundaries [30],[31]. In the electroosmotic flow the fluid is driven due to the electric field. After the fluid comes in contact with microchannel walls, the counter ions in the fluid migrate toward the charged walls and an electric charge gradient prevails near the walls. This ion distribution is described by Boltzmann equation ($n_i = n_{\infty} \exp[z e \psi / (k_b T)]$) [32], where n_i stands for ionic number density of i th ion, n_{∞} denotes ionic number density of bulk flow, z is the absolute value of the ionic valence, e is the fundamental charge of an electron, k_b represents Boltzmann constant, ψ is electrical field potential, and T denotes the absolute temperature in Kelvin. Due to the ionic distribution along the microchannel wall, an electrical layer is formed, in which, charge gradient exist near the wall and ion distribution is uniform in the rest of bulk flow, called electric double layer (EDL), described by the Poisson equation ($(\partial^2 \psi) / (\partial y^2) = \rho_e / (\epsilon \epsilon_0)$) [33]. Where ρ_e is local net charge density per unit volume, ϵ and ϵ_0 are the electrical permittivity constants in the medium and in the vacuum, respectively.

For mathematical modelling of electroosmotic flow, fluid flow and electric field equations must be solved simultaneously, described by Navier-Stokes equations [34] and the Poisson-Boltzmann equations, respectively. In this paper, a rectangular microchannel is considered, the main flow direction is considered in the X direction, while the channel length is L , its height is H , and channel width is W (Fig. 1-a).

In analysis of electroosmotic flow in microchannels generally a fully developed laminar flow along the microchannel can be reasonably considered, because of the low Reynolds number ($RE < 1$) encountered. Moreover, since

the microchannel width is considerably greater than its height ($W \gg H$), changes in velocity and ion density at channel width can be ignored and the problem can be solved 2D.

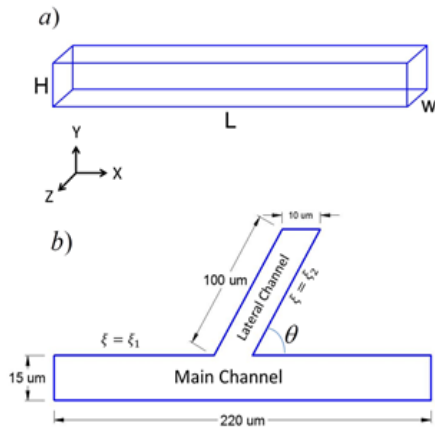


Fig. 1 a) Schematic of the rectangular microchannel considered, b) Dimension of branches, divergence angle and applied zeta potential on microchannel walls (Not in scale)

2.1. Electric Field and Ion Distribution

EDL field manifest its impact on the velocity field through an electric body force in the Navier-Stokes equation. As a result, to determine the flow field, EDL field must be firstly solved to obtain ionic density distribution in the EDL, described by the Boltzman distribution [33]:

$$\rho_e = -2n_\infty ze \sinh\left(\frac{ze\psi}{k_b T}\right) \quad (1)$$

To solve 2-dimensional EDL field in a rectangular microchannel Poisson, equation (Eq. 2) is used [33].

$$\frac{\partial^2 \psi}{\partial y^2} = \frac{\rho_e}{\epsilon \epsilon_0} \quad (2)$$

In this equation, ρ_e is ion density in EDL. By substitution of the Boltzmann equation (Eq. 1) into the Poisson equation, the governing Poisson-Boltzmann equation will be obtained [33]:

$$\frac{\partial^2 \psi}{\partial y^2} = \frac{2n_\infty ze}{\epsilon \epsilon_0} \sinh\left(\frac{ze\psi}{k_b T}\right) \quad (3)$$

Upon solving the Poisson-Boltzmann equation (Eq. 3), the ionic distribution in the microchannel is determined, which will be later used to determine the ion density profile and finally the velocity profile.

2.2. Fluid flow in rectangular microchannel

The Navier-Stokes equations for a fully developed, steady state, and incompressible flow with constant viscosity, and under atmospheric pressure, for a dilute solution is as follows[34]:

$$\mu \left(\frac{\partial^2 u}{\partial y^2} \right) = F_x \quad (4)$$

where F_x denotes the body forces, and equals the product of to the electric field (E_x) and local ion density (ρ_e) [33]:

$$F_x = \rho_e E_x \quad (5)$$

Incorporating Eq. (1) and Eq. (4) in the Eq. (5), the governing velocity field equation will be obtained [33]:

$$\mu \left(\frac{\partial^2 u}{\partial y^2} \right) = \left[2n_\infty ze \sinh\left(\frac{ze\psi}{k_b T}\right) \right] E_x \quad (6)$$

3 NUMERICAL MODEL

For numerical simulations, a rectangular microchannel and its branch is considered with the schematic illustration shown in Fig. 1-b. An electric potential is applied between the inlet and outlet of the main channel and the walls experience ξ_1 and ξ_2 potentials as the boundary conditions (Fig. 1-b). ξ_i is the amount of surface charge accumulated on the microchannel wall.

Differential equations which were explained in the mathematical model section are solved by finite element software Comsol Multiphysics using a 2-dimensional triangular element. To insure independence from the mesh size, sensitivity analysis was performed with "3%" difference threshold. Numerical model is validated and compared with the results published by Bianchi et.al [35], where it is appropriate.

4 RESULTS

To investigate the effect of divergence angle change on the shear rate, the numerical model in 4 branch angles of "60°, 90°, 120° and 150°" was implemented. To facilitate studying the impact of divergence angle change on the flow characteristics, a half-zone (\hat{e}) is defined at the entrance of branch according to Fig. 2 Due to the divergence angle change, many changes in hydrodynamic properties of the flow can be observed in this zone. Here, the length of entrance half-zone is "5 μm ".

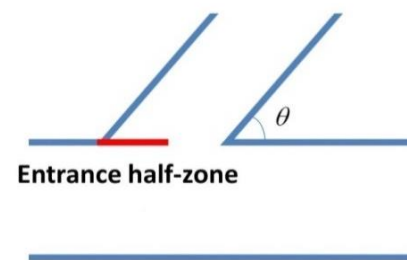


Fig. 2 Schematic of entrance half-zone

Shear rate plays an important role in accessing the health state of cells/proteins upon passing physical obstacles in micro/nano-channel networks. Shear rate is computed by our FEM model at the non-dimensional entrance half-zone for the 4 divergence angles "60, 90, 120 and 150°" and tabulated in Fig. 3 The distance (x) from the branch toward its center is non-dimensionalized by the "5 μ m" entrance half zone ($x^* = x\hat{e}^{-1}$). The shear rate (s^{-1}) is also non-dimensionalized by the critical shear rate of the Red Blood Cells ($s^{-1}_{cr} = 764 \times 10^3 s^{-1}$)[27], above which the cell will be denatured ($s^{-1*} = \frac{s^{-1}}{s^{-1}_{cr}}$).

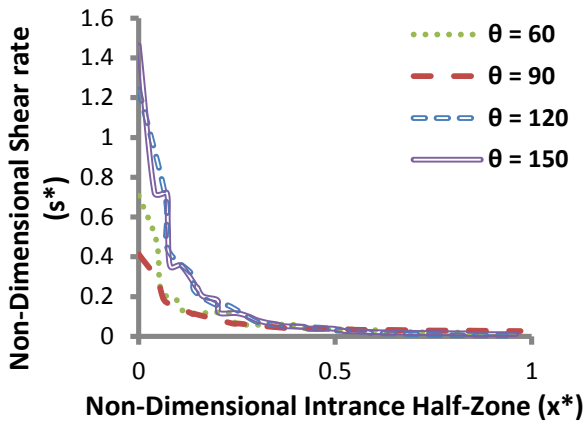


Fig. 3 The non-dimensional shear rate along the entrance half zone of the channel branch for 4 divergence angles "60, 90, 120 and 150°". Increase of branch angle above "90°" results in a sudden increase in the shear rate

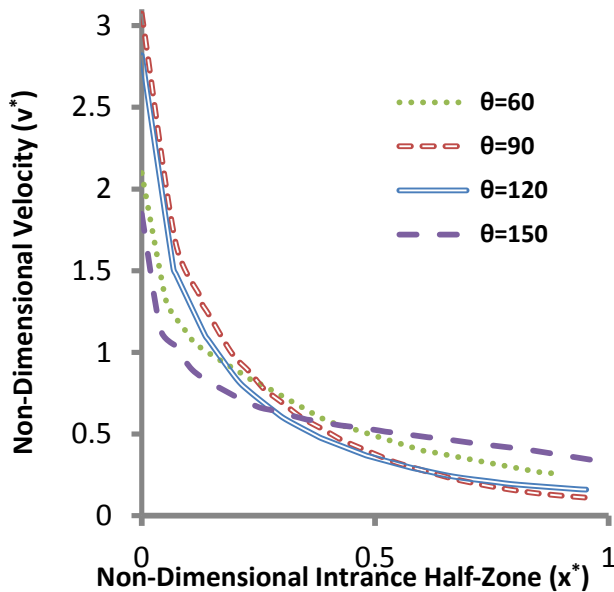


Fig. 4 The non-dimensional Velocity (v^*) through the non-dimensional entrance half zone (x^*) for the 4 divergence angles "60, 90, 120 and 150°" (Change in angle of divergence have no considerable effect on velocity magnitude.)

Figure 3 illustrates that increase of divergence angle above "90°" leads to a significant increase in shear rate. Upon increase of divergence angle from "60°" to "150°", the maximum shear rate shall increase 2.1 times higher than the previous amount. Critical shear rate would denature the red blood cell (RBC) in bloods sample, while entering the branch. One might speculate that change of divergence angle impacts the shear rate due to a sudden change in the velocity magnitude immediately to the entrance half zone. However, Fig. 4 shows that change of divergence angle does not have a considerable impact on the velocity (v^*) magnitude (velocity is non-dimensionalized by the 0.004 mm/s $v^* = v/0.004$). Nevertheless, steep change of velocity direction, and accordingly, deflection of the streamlines would bring about maximum shear imposed on the fluid and suspended particles carried along. This result has a significant importance in prediction of branches and manipulation lines in lab-on-a-chip devices where knowledge of shear rates experience by proteins is required before the fabrication stage.

In addition to the entrance half-zone, shear rate changes significantly at channel walls immediately to the branch. Fig. 5 below depicts the change of shear rate ($s^{-1*} = \frac{s^{-1}}{s_{cr}^{-1}}$) with respect to the non-dimensionalized immediate-Junction Length (L^*). The distance (L) from the Channel walls toward immediate to the branch is non-dimensionalized by the "0.5 μ m" (\hat{a}) Immediate-Junction Length ($L^* = L\hat{a}^{-1}$).

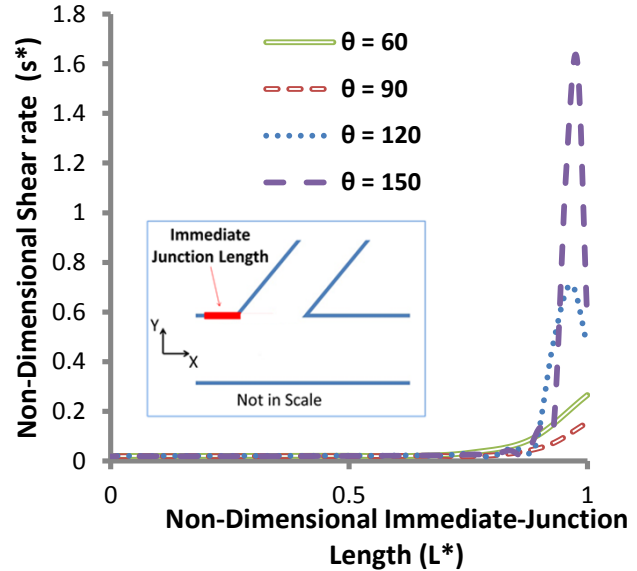


Fig. 5 The Non-dimensional shear rate along the non-dimensional immediate-junction length. The shear rate is non-dimensionalized by the critical shear rate of the red blood cell: $s^{-1}_{cr} = 764 \times 10^3 s^{-1}$ and the distance (L) from Channel walls toward immediate to the branch is non-dimensionalized by the 0.5 μ m (\hat{a}) Immediate-Junction Length ($L^* = L\hat{a}^{-1}$). Wall shear rate remains almost the same along the channel wall expect for branch angles above "90 degrees" were the maximum wall shear rate increases for one order of magnitude for increase of angle from "90 to 150°".

Figure 5 shows that upon increase of branch angle over "90°", there is a sharp increase in the wall shear rate immediate to the branch. This observation is especially important considering the fact that due to intrinsic charge of the proteins, they often tend to stick to the microchannel walls and if the microchannel network has not been carefully designed, any steep divergence angle would definitely result in protein denaturation. For example, the wall shear rate near the branch entrance will increase for around one order of magnitude from 0.3 at 60° to 1.6 at 150°.

To investigate the effect of zeta potential on the tendency of suspended particles to enter the branch, a microchannel with a width of "20µm", at 3 branch angles of "30°, 45° and 60°", and with three $\frac{\xi_1}{\xi_2}$ proportions of 0.5, 1 and 2 is simulated. The velocity profile across the channel width (at the branch), and also, the maximum velocity is recorded. Fig.6 shows the velocity profile at the branch exit cross-section for 3 conditions of $\frac{\xi_1}{\xi_2} = 0.5$, $\frac{\xi_1}{\xi_2} = 1$ and $\frac{\xi_1}{\xi_2} = 2$ and 3 branch angles of "30°, 45° and 60°".

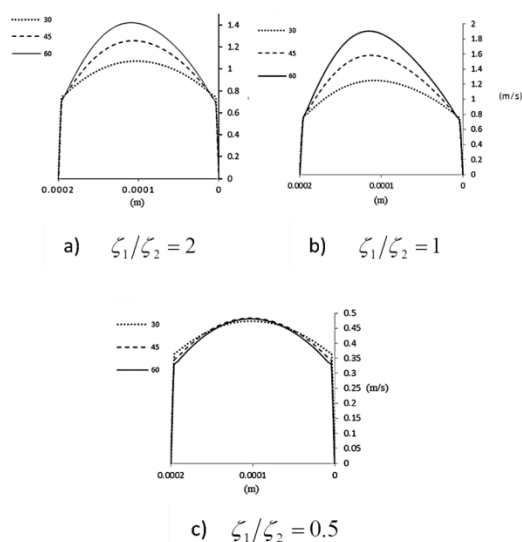


Fig. 6 The velocity profile in outlet section of branch for 3 divergence angles "30, 45 and 60°". In almost any wall electric potential distribution, increase of branch angle results in increase of branch velocity; however, when $\xi_2 = 2\xi_1$ the velocity at the branch is independent from the branch angle

Figure 6 reveals that when branch has more surface charge density than the main channel, the branch angle has negligible effect on the velocity magnitude of the branch. However for any other configuration, increase of branch angle would increase the velocity in the branch, a counter intuitive observation. Presumably, the reason behind this observation is the fact that the fluid driving force is the surface charge density whether on branch or main microchannel walls. As a result, the head lost which

becomes prevalent with increase of branch angle, in pressure driven flows, is absent here.

Particles' tendency to enter the branch can be correlated to the increase of maximum velocity at the branch. This speculation is reasonable for dilute solutions, where the solute does not affect the flow pattern, since the suspended particles closely follow the flow pattern. Fig. 7 below, shows that for any electrical potential on the walls except for the $\frac{\xi_1}{\xi_2} = 0.5$, increase of branch angle results increase of maximum velocity and as a result, increase of particles tendency to enter the branch.

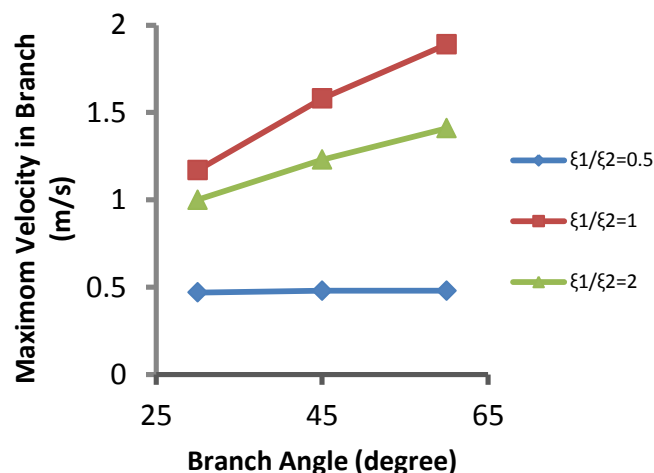


Fig. 7 Increase of branch angle results in increase of maximum velocity in the branch. The branch Maximum velocity is plotted for three zeta potential ratios and for three branch angles.

Figure 7 also shows that for $\frac{\xi_1}{\xi_2} = 1$, case of uniform charge density distribution over microchannel walls and branch, increase of divergence angle results in increase of maximum velocity in the branch. Therefore, in this case, the particles tendency to pass through the branch increases upon increase of branch angle.

5 CONCLUSION

Through numerical simulations we have demonstrated that increase of branch angle to more than 90°, results in a significant increase in the shear rate immediate to the branching zone and the microchannel walls. In more details, upon increase of branch angle from "60° to 90°", the shear rate increases for 210%. This observation is practically important, since due to numerous applications of electroosmotic flows in transport and control of biologic samples, existence of multiple branches is inevitable and improper design of these microfluidic networks would result in denaturation of different cells and proteins. Moreover, we

have shown that the tendency of particles to enter branches generally increases with increase of branch angles.

ACKNOWLEDGMENTS

This research was financially supported by the Ministry of Science, Research and Technology (MSRT), Iran. The authors would like to acknowledge the products and services provided by MSRT that facilitated this research.

REFERENCES

- [1] W. L. W. Hau, D. W. Trau, N. J. Sucher, M. Wong, and Y. Zohar, "Surface-chemistry technology for microfluidics," *J. micromechanics microengineering*, vol. 13, no. 2, p. 272, 2003.
- [2] A. D. Stroock, M. Weck, D. T. Chiu, W. T. S. Huck, P. J. A. Kenis, R. F. Ismagilov, and G. M. Whitesides, "Patterning electro-osmotic flow with patterned surface charge," *Phys. Rev. Lett.*, vol. 84, no. 15, p. 3314, 2000.
- [3] Y. Takamura, H. Onoda, H. Inokuchi, S. Adachi, A. Oki, and Y. Horiike, "Low-voltage electroosmosis pump for stand-alone microfluidics devices," *Electrophoresis*, vol. 24, no. 1-2, pp. 185–192, 2003.
- [4] L. Bousse, C. Cohen, T. Nikiforov, A. Chow, A. R. Kopf-Sill, R. Dubrow, and J. W. Parce, "Electrokinetically controlled microfluidic analysis systems," *Annu. Rev. Biophys. Biomol. Struct.*, vol. 29, no. 1, pp. 155–181, 2000.
- [5] A. Ajdari, "Transverse electrokinetic and microfluidic effects in micropatterned channels: Lubrication analysis for slab geometries," *Phys. Rev. E*, vol. 65, no. 1, p. 16301, 2001.
- [6] L. M. Lee, W. L. W. Hau, Y.-K. Lee, and Y. Zohar, "In-plane vortex flow in microchannels generated by electroosmosis with patterned surface charge," *J. micromechanics microengineering*, vol. 16, no. 1, p. 17, 2006.
- [7] A. S. W. Ng, W. L. W. Hau, Y.-K. Lee, and Y. Zohar, "Electrokinetic generation of microvortex patterns in a microchannel liquid flow," *J. micromechanics microengineering*, vol. 14, no. 2, p. 247, 2004.
- [8] G. Whitesides and A. Stroock, "Flexible methods for microfluidics [J]," *Phys Today*, vol. 54, no. 6, pp. 42–48, 2001.
- [9] H. A. Stone, A. D. Stroock, and A. Ajdari, "Engineering flows in small devices: microfluidics toward a lab-on-a-chip," *Annu. Rev. Fluid Mech.*, vol. 36, pp. 381–411, 2004.
- [10] D. Marro, Y. N. Kalia, M. B. Delgado-Charro, and R. H. Guy, "Contributions of electromigration and electroosmosis to iontophoretic drug delivery," *Pharm. Res.*, vol. 18, no. 12, pp. 1701–1708, 2001.
- [11] C. Wiles and P. Watts, "Improving chemical synthesis using flow reactors," 2007.
- [12] A. K. Vijh, "Electrochemical treatment of tumors (ECT): electroosmotic dewatering (EOD) as the primary mechanism," *Dry. Technol.*, vol. 17, no. 3, pp. 586–596, 1999.
- [13] S. T. P. YK Ng E, "CFD analysis of double-layer microchannel conjugate parallel liquid flows with electric double-layer effects," *Numer. Heat Transf. Part A Appl.*, vol. 40, no. 7, pp. 735–749, 2001.
- [14] E. Y. K. Ng and S. T. Tan, "Computation of three-dimensional developing pressure-driven liquid flow in a microchannel with EDL effect," *Numer. Heat Transf. Part A*, vol. 45, no. 10, pp. 1013–1027, 2004.
- [15] S. T. Tan and E. Y. K. Ng, "Numerical analysis of EDL effect on heat transfer characteristic of 3-D developing flow in a microchannel," *Numer. Heat Transf. Part A Appl.*, vol. 49, no. 10, pp. 991–1007, 2006.
- [16] E. Y. K. Ng and S. T. Tan, "Study of EDL effect on 3-D developing flow in microchannel with Poisson-Boltzmann and Nernst-Planck models," *Int. J. Numer. Methods Eng.*, vol. 71, no. 7, pp. 818–836, 2007.
- [17] H. Andersson, W. Van Der Wijngaart, P. Nilsson, P. Enoksson, and G. Stemme, "A valve-less diffuser micropump for microfluidic analytical systems," *Sensors Actuators B Chem.*, vol. 72, no. 3, pp. 259–265, 2001.
- [18] T. E. McKnight, C. T. Culbertson, S. C. Jacobson, and J. M. Ramsey, "Electroosmotically induced hydraulic pumping with integrated electrodes on microfluidic devices," *Anal. Chem.*, vol. 73, no. 16, pp. 4045–4049, 2001.
- [19] P. C. H. Li and D. J. Harrison, "Transport, manipulation, and reaction of biological cells on-chip using electrokinetic effects," *Anal. Chem.*, vol. 69, no. 8, pp. 1564–1568, 1997.
- [20] S. Ebrahimi, A. Hasanzadeh-Barforoushi, A. Nejat, and F. Kowsary, "Numerical study of mixing and heat transfer in mixed electroosmotic/pressure driven flow through T-shaped microchannels," *Int. J. Heat Mass Transf.*, vol. 75, pp. 565–580, 2014.
- [21] A. Soleymani, E. Kolehmainen, and I. Turunen, "Numerical and experimental investigations of liquid mixing in T-type micromixers," *Chem. Eng. J.*, vol. 135, pp. S219–S228, 2008.
- [22] Y. Ai, S. Park, J. Zhu, X. Xuan, A. Beskok, and S. Qian, "DC electrokinetic particle transport in an L-shaped microchannel," *Langmuir*, vol. 26, no. 4, pp. 2937–2944, 2009.
- [23] S. Bhopte, B. Sammakia, and B. Murray, "Geometric modifications to simple microchannel design for enhanced mixing," in 2008 11th IEEE Intersociety Conference on Thermal and Thermomechanical Phenomena in Electronic Systems, I-THERM, 2008, pp. 937–944.
- [24] E. A. Mansur, 王运东, 戴贻元, E. A. Mansur, W. Yundong, and D. A. I. You-yuan, "Computational fluid dynamic simulation of liquid-liquid mixing in a static double-T-shaped micromixer," *过程工程学报* vol. 8, no. 6, 2008.
- [25] J. G. Santiago, "Electroosmotic flows in microchannels with finite inertial and pressure forces," *Anal. Chem.*, vol. 73, no. 10, pp. 2353–2365, 2001.
- [26] E. J. Lim, T. J. Ober, J. F. Edd, S. P. Desai, D. Neal, K. W. Bong, P. S. Doyle, G. H. McKinley, and M. Toner, "Inertio-elastic focusing of bioparticles in microchannels at high throughput," *Nat. Commun.*, vol. 5, p. 4120, 2014.
- [27] L. B. Leverett, J. D. Hellums, C. P. Alfrey, and E. C. Lynch, "Red blood cell damage by shear stress," *Biophys. J.*, vol. 12, no. 3, p. 257, 1972.
- [28] O. K. Baskurt, "Red blood cell mechanical stability," *Engineering*, vol. 4, no. 10, p. 8, 2013.
- [29] G. M. Yezaz Ahmed and A. Singh, "Numerical simulation of particle migration in asymmetric bifurcation channel," *J. Nonnewton. Fluid Mech.*, vol. 166, no. 1–2, pp. 42–51, 2011.

- [30] A. N. Frumkin, O. A. Petrii, B. B. Damaskin, J. O. M. Bockris, B. E. Conway, and E. Yeager, "Comprehensive Treatise of Electrochemistry," Vol. 1 Plenum, New York, pp. 246–251, 1980.
- [31] F. F. Reuss, "Sur un nouvel effet de l'électricité galvanique," Mem. Soc. Imp. Natur. Moscou, vol. 2, pp. 327–337, 1809.
- [32] H. Bruus, *Theoretical Microfluidics*. OUP Oxford, 2008.
- [33] D. Li, *Electrokinetics in Microfluidics*. Academic, 2004.
- [34] R. H. Pletcher, J. C. Tannehill, and D. Anderson, *Computational Fluid Mechanics and Heat Transfer*, Third Edition. CRC Press, 2012.
- [35] F. Bianchi, R. Ferrigno, and H. H. Girault, "Finite element simulation of an electroosmotic-driven flow division at a T-junction of microscale dimensions," *Anal. Chem.*, vol. 72, no. 9, pp. 1987–1993, 2000.